

TRANSIENT RESPONSE OF AN INHOMOGENEOUS ELASTIC SOLID TO A MOVING TORSIONAL LOAD IN A CYLINDRICAL BORE

KAZUMI WATANABE

Department of Mechanical Engineering, Technical College, Yamagata University,
Yonezawa, Yamagata 992, Japan

(Received 2 June 1983)

Abstract—The transient response of an inhomogeneous elastic solid to a torsional ring load is considered. The load is suddenly applied to a cylindrical wall in the solid and then moves along a bore. The inhomogeneity of the solid is assumed as $\mu/\mu_0 = \rho/\rho_0 = (r/a)^k$, so that SH-wave velocity is constant throughout the solid.

A general form of solution is obtained for an arbitrary motion of the load. It can be applicable to both transient and steady-state problems of the moving/stationary load. Explicit expressions for the displacement are given for three types of the load applications; (a) impulsive load, (b) step pulse load, (c) uniformly moving load. Numerical computations are carried out for the displacement in detail. The displacement singularities at wave fronts and beneath the loaded point are also discussed.

INTRODUCTION

The dynamical problem of an elastic solid with a cylindrical bore has considerable importances in engineering however, the response of the bored elastic solid to a moving load has been less studied. The presence of the cylindrical bore causes the dispersion of wave and then the mathematical treatment for these problems becomes so complex. It seems that the researches in this area are limited only to the steady-state problems in a homogeneous elastic solid. Parnes[1] presented an analytical procedure for non-axisymmetric problems of normal, tangential and torsional loads moving superseismically in a cylindrical bore, but numerical computations were carried out only for the axisymmetric case of the normal load. The problem of a moving torsional load was also discussed by him[2], where numerical computations were carried out in detail for subseismic, seismic and superseismic velocities of the load.

Excepting Parnes's works, we cannot find any contribution to the problem of the moving load in the bored elastic solid. Of course, no transient problems of this type were there. The present paper considers the transient response of an inhomogeneous elastic solid to a moving torsional load in a cylindrical bore. Its inhomogeneity is assumed that rigidity μ and mass density ρ vary only with radial distance r so that SH-wave velocity is constant throughout the solid. A general form of solution, which is applicable to both transient and steady-state problems of the dynamic load, is obtained for two cases of the inhomogeneity. One is that the rigidity and the density increase linearly with the radial distance and the other is inverse of the former. Explicit expressions of the displacement are obtained for three types of the loading; (a) impulsive load, (b) step pulse load, (c) uniformly moving load. Numerical computations for the displacement response are carried out in detail and the singularities at the wave fronts and beneath the loaded point are discussed. It is shown from the figures that a valley of the deformation is found only in the increasing case of the material parameters. The effect of the inhomogeneity on the response fades out with increasing of Mach number of the moving load.

Aside from the academic interest and possible application of the inhomogeneity assumed here, the present solution is exact and could possibly be used for assessing the accuracy of approximate methods of solutions in elasto-dynamic problems.

STATEMENT OF PROBLEM

Consider a cylindrical bore of radius a in an inhomogeneous elastic solid and take a cylindrical coordinate system (r, θ, z) whose z -axis lies on the axis of the bore (Fig. 1).

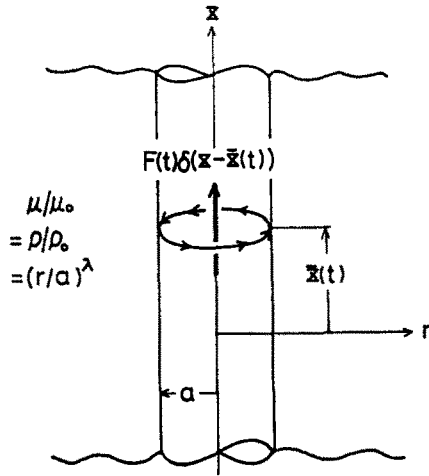


Fig. 1. Moving torsional ring load in a cylindrical bore.

A torsional ring load is suddenly applied to the surface of the bore and then moves along it. It is also assumed that the distribution of the load is symmetric about the z -axis. Non-vanishing components of stress and displacement are $\sigma_{r\theta}$, $\sigma_{z\theta}$ and U_θ . Equation of motion and constitutive equations are given by

$$\sigma_{r\theta,r} + \frac{2}{r}\sigma_{r\theta} + \sigma_{z\theta,r} = \rho U_{\theta,tt} \tag{1}$$

$$\sigma_{r\theta} = \mu \left(U_{\theta,r} - \frac{1}{r}U_\theta \right), \quad \sigma_{z\theta} = \mu U_{\theta,z} \tag{2}$$

where rigidity μ and mass density ρ vary only with radial distance r .

$$\mu/\mu_0 = \rho/\rho_0 = (r/a)^\lambda \tag{3}$$

where subscript 0 stands for the quantities at the cylindrical wall, $r = a$, and constant λ is an inhomogeneous parameter to be specified later. Equation (3) states that SH-wave velocity is constant throughout the solid. That is

$$c = (\mu/\rho)^{1/2} = (\mu_0/\rho_0)^{1/2}. \tag{4}$$

We shall assume that the magnitude and position of the moving load are to be time-dependent and are expressed by $F(t)$ and $\bar{z}(t)$, respectively. The boundary condition at the cylindrical wall is given by

$$\sigma_{r\theta} = F(t)\delta(z - \bar{z}(t))H(t) ; r = a \tag{5}$$

where $\delta(\cdot)$ and $H(\cdot)$ are Dirac's delta and Heaviside's unit step functions, respectively.

A radiation condition at infinity, $r \rightarrow \infty$,

$$U_\theta \rightarrow 0 ; r \rightarrow \infty \tag{6}$$

and a quiescent condition at initial time, $t = 0$,

$$U_\theta = U_{\theta,t} = 0 ; t = 0 \tag{7}$$

are also employed.

GENERAL PROCEDURES

Let us introduce the following non-dimensionalizations;

$$\xi = r/a, \zeta = z/a, \tau = ct/a \tag{8}$$

$$F(\tau) \equiv F(a\tau/c), l(\tau) = \bar{z}(a\tau/c)/a \tag{9}$$

Substituting eqn (8) and (9) together with eqn (2) into eqn (1), we get the displacement equation as

$$\frac{\partial^2 U_\theta}{\partial \xi^2} + \frac{\lambda + 1}{\xi} \cdot \frac{\partial U_\theta}{\partial \xi} + \frac{\lambda + 1}{\xi^2} U_\theta + \frac{\partial^2 U_\theta}{\partial \zeta^2} = \frac{\partial^2 U_\theta}{\partial \tau^2} \tag{10}$$

Applying the integral transforms,
Fourier transform:

$$\tilde{f}(\eta) = \int_{-\infty}^{\infty} f(\zeta) \exp(i\eta\zeta) d\zeta, f(\tau) = \frac{1}{2\pi} \int_{-\infty}^{\infty} \tilde{f}(\eta) \exp(-i\eta\zeta) d\eta \tag{11}$$

and Laplace transform:

$$f^*(s) = \int_0^{\infty} f(\tau) \exp(-s\tau) d\tau, f(\tau) = \frac{1}{2\pi i} \int_{B_r} f^*(s) \exp(s\tau) ds \tag{12}$$

to eqn (10), we have the transformed solution as

$$\tilde{U}_\theta^* = \xi^{-\lambda/2} \{C_1 I_\nu(\beta\xi) + C_2 K_\nu(\beta\xi)\} \tag{13}$$

$$\frac{a}{\mu} \tilde{\sigma}_{r\theta}^* = \beta\xi^{-\lambda/2} \{C_1 I_{\nu+1}(\beta\xi) - C_2 K_{\nu+1}(\beta\xi)\} \tag{14}$$

$$\frac{a}{\mu} \tilde{\sigma}_{z\theta}^* = -i\eta\xi^{-\lambda/2} \{C_1 I_\nu(\beta\xi) + C_2 K_\nu(\beta\xi)\} \tag{15}$$

where

$$\nu = \lambda/2 + 1 \tag{16}$$

$$\beta = (\xi^2 + s^2)^{1/2}; \text{Re}(\beta) > 0 \tag{17}$$

and $I_\nu()$ and $K_\nu()$ are the modified Bessel functions of the first and second kinds, respectively. $C_j (j = 1, 2)$ are unknown coefficients to be determined by the conditions,

$$\tilde{\sigma}_{r\theta}^* = \frac{1}{a} \int_0^\infty F(u) \exp\{i\eta l(u) - su\} du ; \xi = 1 \tag{18}$$

$$\tilde{U}_\theta^* = 0 ; \xi \rightarrow \infty \tag{19}$$

Equation (19) states $C_1 = 0$ and eqn (18) demands

$$C_2 = -\frac{1}{\mu_0 \beta K_{\nu+1}(\beta)} \int_0^\infty F(u) \exp\{i\eta l(u) - su\} du \tag{20}$$

Then, the transformed displacement yields

$$\tilde{U}_\theta^* = -\frac{\xi^{-\lambda/2}}{\mu_0 \beta} \frac{K_\nu(\beta\xi)}{K_{\nu+1}(\beta)} \int_0^\infty F(u) \exp\{i\eta l(u) - su\} du \tag{21}$$

Stresses will be obtained easily with substitution of eqn (20) into eqns (14) and (15).

We shall consider an inversion of the transformed displacement given by eqn (21). Two cases of the inhomogeneous parameter are discussed,

Case A: $\lambda = 1, \nu = \frac{3}{2}$

Case B: $\lambda = -1, \nu = \frac{1}{2}$.

In both cases, the order of the Bessel function in eqn (21) is half of an odd integer. In Case A, we can use the simple expressions of the Bessel function ([3], p. 80),

$$K_{3/2}(z) = \sqrt{\frac{\pi}{2z}} \left(1 + \frac{1}{z}\right) \exp(-z) \tag{22a}$$

$$K_{5/2}(z) = \sqrt{\frac{\pi}{2z}} \left(1 + \frac{3}{z} + \frac{3}{z^2}\right) \exp(-z). \tag{22b}$$

Substituting eqn (22) into eqn (21) and manipulating, we get

$$\begin{aligned} \bar{U}_0 = & -\frac{1}{2\mu_0\xi} \int_0^\infty F(u) \left(\frac{1}{\beta+p} + \frac{1}{\beta+q}\right) \exp\{i\eta l(u) - \beta\bar{\xi} - su\} du \\ & - \frac{i\sqrt{3}}{3\mu_0\xi} \left(\frac{1}{\xi} - \frac{3}{2}\right) \int_0^\infty F(u) \left(\frac{1}{\beta+p} - \frac{1}{\beta+q}\right) \exp\{i\eta l(u) - \beta\bar{\xi} - su\} du \end{aligned} \tag{23}$$

where

$$\bar{\xi} = \xi - 1, \tag{24}$$

$$\begin{pmatrix} p \\ q \end{pmatrix} = (3 \pm i\sqrt{3})/2. \tag{25}$$

Now, applying Laplace inversion formula ([14], Appendix),

$$\begin{aligned} L^{-1} \left\{ \frac{\exp(-\bar{\xi}\sqrt{\eta^2 + s^2} - su)}{\alpha + \sqrt{\eta^2 + s^2}} \right\} = & H(\tau - u - \bar{\xi}) \left[J_0(\eta\sqrt{(\tau - u)^2 - \bar{\xi}^2}) \right. \\ & \left. - \alpha \int_0^{\sqrt{(\tau - u)^2 - \bar{\xi}^2}} \frac{x}{\sqrt{(\tau - u)^2 - x^2}} J_0(\eta x) \exp\{-\alpha(\sqrt{(\tau - u)^2 - x^2} - \bar{\xi})\} dx \right] \end{aligned} \tag{26}$$

where α takes p or q and $J_0(\cdot)$ is Bessel function of the first kind, to eqn (23), we get

$$\begin{aligned} \bar{U}_0 = & -\frac{1}{\mu_0\xi} \int_0^\infty H(\tau - u - \bar{\xi}) F(u) \exp\{i\eta l(u)\} \left[J_0(\eta\sqrt{(\tau - u)^2 - \bar{\xi}^2}) \right. \\ & \left. - \frac{1}{2} \int_{\bar{\xi}}^{\tau - u} \left[3 \cos\left\{\frac{\sqrt{3}}{2}(x - \bar{\xi})\right\} + \sqrt{3} \sin\left\{\frac{\sqrt{3}}{2}(x - \bar{\xi})\right\} \right] \right. \\ & \left. \times J_0(\eta\sqrt{(\tau - u)^2 - x^2}) \exp\left\{-\frac{3}{2}(x - \bar{\xi})\right\} dx \right] du - \frac{1}{\mu_0\xi} \\ & \times \left(\frac{1}{\xi} - \frac{3}{2}\right) \int_0^\infty H(\tau - u - \bar{\xi}) F(u) \exp\{i\eta l(u)\} \left[\int_{\bar{\xi}}^{\tau - u} \left[\cos\left\{\frac{\sqrt{3}}{2}(x - \bar{\xi})\right\} \right. \right. \\ & \left. \left. - \sqrt{3} \sin\left\{\frac{\sqrt{3}}{2}(x - \bar{\xi})\right\} \right] J_0(\eta\sqrt{(\tau - u)^2 - x^2}) \exp\left\{-\frac{3}{2}(x - \bar{\xi})\right\} dx \right] du. \end{aligned} \tag{27}$$

The formal Fourier inversion is defined by

$$U_\theta = \frac{1}{2\pi} \int_{-\infty}^{\tau} \tilde{U}_\theta \exp(-i\eta\zeta) d\eta. \tag{28}$$

Substituting eqn (27) into eqn (28) and changing the order of integration, we have

$$\begin{aligned} U_\theta = & -\frac{1}{\mu_0 \bar{\xi}} \int_0^\infty H(\tau - u - \bar{\xi}) F(u) \left[\left[\Phi(\sqrt{(\tau - u)^2 - \bar{\xi}^2}, \zeta - l(u)) \right. \right. \\ & - \frac{1}{2} \int_{\bar{\xi}}^{\tau - u} \left[3 \cos\left\{ \frac{\sqrt{3}}{2}(x - \bar{\xi}) \right\} + 3 \sin\left\{ \frac{\sqrt{3}}{2}(x - \bar{\xi}) \right\} \right] \\ & \times \Phi(\sqrt{(\tau - u)^2 - x^2}, \zeta - l(u)) \exp\left\{ -\frac{3}{2}(x - \bar{\xi}) \right\} dx \left. \right] du \\ & - \frac{1}{\mu_0 \bar{\xi}} \left(\frac{1}{\bar{\xi}} - \frac{3}{2} \right) \int_0^\infty H(\tau - u - \bar{\xi}) F(u) \left[\left[\int_{\bar{\xi}}^{\tau - u} \left[\cos\left\{ \frac{\sqrt{3}}{2}(x - \bar{\xi}) \right\} \right] \right. \right. \\ & + \sqrt{3} \sin\left\{ \frac{\sqrt{3}}{2}(x - \bar{\xi}) \right\} \left. \right] \Phi(\sqrt{(\tau - u)^2 - x^2}, \zeta - l(u)) \\ & \times \exp\left\{ -\frac{3}{2}(x - \bar{\xi}) \right\} dx \left. \right] du \end{aligned} \tag{29}$$

where

$$\Phi(a, b) = \frac{1}{2\pi} \int_0^\infty J_0(\eta a) \exp(-i\eta b) d\eta. \tag{30}$$

Equation (30) is easily evaluated as

$$\Phi(a, b) = \frac{H(|a| - |b|)}{\pi \sqrt{a^2 - b^2}}. \tag{31}$$

Then, the final form of the displacement yields

$$\begin{aligned} U_\theta = & -\frac{1}{\pi \mu_0 \bar{\xi}} \int_0^\infty H(\tau - T(u)) F(u) \left[\left[\frac{1}{\sqrt{(\tau - u)^2 - \bar{\xi}^2 - \{\zeta - l(u)\}^2}} \right. \right. \\ & - \int_{\bar{\xi}}^{\sqrt{(\tau - u)^2 - \{\zeta - l(u)\}^2}} \frac{\exp\{-3(x - \bar{\xi})/2\}}{\sqrt{(\tau - u)^2 - x^2 - \{\zeta - l(u)\}^2}} \\ & \times \left(3 - \frac{1}{\bar{\xi}} \right) \cos\left\{ \frac{\sqrt{3}}{2}(x - \bar{\xi}) \right\} - \sqrt{3} \left(1 - \frac{1}{\bar{\xi}} \right) \sin\left\{ \frac{\sqrt{3}}{2}(x - \bar{\xi}) \right\} dx \left. \right] du \end{aligned} \tag{32}$$

where $T(u)$ is an arrival time function given by

$$T(u) = u + \sqrt{\bar{\xi}^2 + \{\zeta - l(u)\}^2} \tag{33}$$

and its significance is discussed in [5].

The similar inversion procedure is used for Case B. That is

$$\begin{aligned} U_\theta = & -\frac{1}{\pi \mu_0} \int_0^\infty H(\tau - T(u)) F(u) \left[\frac{1}{\sqrt{(\tau - u)^2 - \bar{\xi}^2 - \{\zeta - l(u)\}^2}} \right. \\ & \left. - \int_{\bar{\xi}}^{\sqrt{(\tau - u)^2 - \{\zeta - l(u)\}^2}} \frac{\exp\{-(x - \bar{\xi})\}}{\sqrt{(\tau - u)^2 - x^2 - \{\zeta - l(u)\}^2}} dx \right] du. \end{aligned} \tag{34}$$

DISCUSSIONS

The transient response of an inhomogeneous elastic solid to a moving load is determined by eqns (32) and (34). Throughout the inversion process, no restrictions were given to the load motion $l(u)$. Therefore, eqns (32) and (34) are the general solutions for the problem of the moving torsional load.

For the convenience of the discussion, we shall summarize eqns (32) and (34) in single form. That is

$$U_{\theta j} = -\frac{C_j}{\pi\mu_0} \int_0^\infty H(\tau - T(u))F(u) \left[\frac{1}{\sqrt{(\tau - u)^2 - \xi^2 - \{\zeta - l(u)\}^2}} - \int_{\bar{\xi}}^{\sqrt{(\tau - u)^2 - \{\zeta - l(u)\}^2}} \frac{G_j(x - \bar{\xi}, \xi)}{\sqrt{(\tau - u)^2 - x^2 - \{\zeta - l(u)\}^2}} dx \right] du \quad (35)$$

where

$$C_A = 1/\xi, \quad C_B = 1 \quad (36)$$

$$G_A(x, y) = \left\{ \left(3 - \frac{1}{y} \right) \cos\left(\frac{\sqrt{3}}{2}x\right) - \sqrt{3} \left(1 - \frac{1}{y} \right) \sin\left(\frac{\sqrt{3}}{2}x\right) \right\} \exp(-3x/2) \quad (37)$$

$$G_B(x, y) = \exp(-x) \quad (38)$$

and subscripts $j = A$ and B stand for Cases A and B , respectively.

Equation (35) states that the integrand with respect to variable u shows the disturbance caused by the load located at time u and that the response at time τ is given as sum up of the disturbance caused at each time u . Then, extending the lower limit of the integral from 0 to $-\infty$, we can obtain another form of the solution, that is applicable not only to the transient problem but also to the steady-state problem of the torsional ring load. That is

$$U_{\theta j} = -\frac{C_j}{\pi\mu_0} \int_{-\infty}^\infty H(\tau - T(u))F(u) \left[\frac{1}{\sqrt{(\tau - u)^2 - \xi^2 - \{\zeta - l(u)\}^2}} - \int_{\bar{\xi}}^{\sqrt{(\tau - u)^2 - \{\zeta - l(u)\}^2}} \frac{G_j(x - \bar{\xi}, \xi)}{\sqrt{(\tau - u)^2 - x^2 - \{\zeta - l(u)\}^2}} dx \right] du. \quad (39)$$

In this solution, the loading condition is given by

$$\sigma_{\theta\theta}|_{r=a} = \frac{1}{a} F(\tau) \delta(\zeta - l(\tau)) \quad (40)$$

where

$$-\infty < \tau < \infty. \quad (41)$$

As an example, we consider a steady-state problem of a stationary load,

$$F(\tau) = F_0 \exp(i\omega\tau), \quad l(\tau) = 0 \quad (42)$$

where ω is a dimensionless frequency. Substituting eqn (42) into eqn (39) and changing the order of integration, we can evaluate the integral with respect to variable u . Then, the steady-state response of displacement is expressed as

$$\frac{2\mu_0}{F_0} U_{\theta j} = iC_j \exp(i\omega\tau) \left\{ H_0^{(2)}(\omega R_0) - \int_{\bar{\xi}}^\infty G_j(x - \bar{\xi}, \xi) H_0^{(2)}(\omega R_x) dx \right\} \quad (43)$$

where $H_0^{(2)}(\cdot)$ is Hankel function of the second kind and

$$R_0 = \sqrt{\bar{\xi}^2 + \zeta^2}, R_x = \sqrt{x^2 + \zeta^2}. \tag{44}$$

NUMERICAL EXAMPLES

Numerical computations are carried out for three combinations of the loading functions;

(a) Impulsive load: $F(\tau) = F_0\delta(\tau), l(\tau) = 0$ (45)

(b) Step pulse load: $F(\tau) = F_0H(\tau), l(\tau) = 0$ (46)

(c) Moving load: $F(\tau) = F_0H(\tau), l(\tau) = M\tau$ (47)

where F_0 is the magnitude of the load and M is the Mach number.

Substituting these loading functions into eqn (39), we can evaluate the integral with respect to variable u . Then the displacement for each loading is obtained as

(a) *Impulsive load*

$$-\frac{\pi\mu_0}{F_0}U_{\theta j} = C_j H(\tau - R_0) \left\{ \frac{1}{\sqrt{\tau^2 - R_0^2}} - \int_{\bar{\xi}}^{\sqrt{\tau^2 - \zeta^2}} \frac{G(x - \bar{\xi}, \xi)}{\sqrt{\tau^2 - R_x^2}} dx \right\}. \tag{48}$$

(b) *Step pulse load*

$$-\frac{\pi\mu_0}{F_0}U_{\theta j} = C_j H(\tau - R_0) \left\{ \cosh^{-1}\left(\frac{\tau}{R_0}\right) - \int_{\bar{\xi}}^{\sqrt{\tau^2 - \zeta^2}} \cosh^{-1}\left(\frac{\tau}{R_x}\right) G(x - \bar{\xi}, \xi) dx \right\}. \tag{49}$$

(c) *Moving load*

(c - 1) subseismic velocity ($0 \leq M < 1$)

$$-\frac{\pi\mu_0}{F_0}U_{\theta j} = \frac{C_j}{\sqrt{1 - M^2}} H(\tau - R_0) \left\{ \log\left(\frac{\sqrt{v_0^+} + \sqrt{v_0^-}}{\sqrt{v_0^+} - \sqrt{v_0^-}}\right) - \int_{\bar{\xi}}^{\sqrt{\tau^2 + \zeta^2}} \log\left(\frac{\sqrt{v_x^+} + \sqrt{v_x^-}}{\sqrt{v_x^+} - \sqrt{v_x^-}}\right) G(x - \bar{\xi}, \xi) dx \right\} \tag{50}$$

where

$$v_0^{\pm} = \tau - M\zeta \pm \sqrt{(\tau - M\zeta)^2 - (1 - M^2)(\tau^2 - R_0^2)} \tag{51}$$

$$v_x^{\pm} = \tau - M\zeta \pm \sqrt{(\tau - M\zeta)^2 - (1 - M^2)(\tau^2 - R_x^2)}. \tag{52}$$

(c - 2) seismic velocity ($M = 1$)

$$-\frac{\pi\mu_0}{F_0}U_{\theta j} = \frac{C_j}{\tau - \zeta} H(\tau - R_0) \left\{ \sqrt{\tau^2 - R_0^2} - \int_{\bar{\xi}}^{\sqrt{\tau^2 - \zeta^2}} \sqrt{\tau^2 - R_x^2} G(x - \bar{\xi}, \xi) dx \right\}. \tag{53}$$

(c - 3) superseismic velocity ($1 < M$)

$$-\frac{\pi\mu_0}{F_0}U_{\theta j} = \frac{C_j}{\sqrt{M^2 - 1}} H(\tau - R_0) \left\{ \frac{\pi}{2} - \tan^{-1} \chi_0 - \int_{\bar{\xi}}^{\sqrt{\tau^2 - \zeta^2}} \left(\frac{\pi}{2} - \tan^{-1} \chi_x \right) \times G(x - \bar{\xi}, \xi) dx \right\} + \frac{C_j}{\sqrt{M^2 - 1}} H(\tau - \tau^*) H(R_0 - \tau) \times H\left(\zeta - \frac{\bar{\xi}}{\sqrt{M^2 - 1}}\right) I_0(\tau_m, \xi) \tag{54}$$

where

$$\chi_0 = \frac{\tau - M\zeta + \sqrt{(\tau - M\zeta)^2 + (M^2 - 1)(\tau^2 - R_0^2)}}{M\zeta - \tau + \sqrt{(\tau - M\zeta)^2 + (M^2 - 1)(\tau^2 - R_0^2)}} \tag{55}$$

$$\chi_x = \frac{\tau - M\zeta + \sqrt{(\tau - M\zeta)^2 + (M^2 - 1)(\tau^2 - R_x^2)}}{M\zeta - \tau + \sqrt{(\tau - M\zeta)^2 + (M^2 - 1)(\tau^2 - R_x^2)}} \tag{56}$$

$$\tau^* = (\zeta + \xi\sqrt{M^2 - 1})/M \tag{57}$$

$$\tau_m = \frac{M}{\sqrt{M^2 - 1}}(\tau - \tau^*) \tag{58}$$

$$I_A(x, y) = \left\{ \cos\left(\frac{\sqrt{3}}{2}x\right) - \sqrt{3}\left(1 - \frac{2}{3y}\right) \sin\left(\frac{\sqrt{3}}{2}x\right) \right\} \exp(-3x/2) \tag{59}$$

$$I_B(x, y) = \exp(-x). \tag{60}$$

In the above examples, the displacement is given in the form of single integration. Numerical computations are very easy. Now, introducing the dimensionless displacement as

$$v = -\frac{\pi\mu_0}{F_0} U_\theta \tag{61}$$

we carried out the computations for the three loading cases and their results are shown in Figs. 2-11.

Figures 2 and 3 are for the case of the impulsive load. Figure 2 shows the displacement response at some observing points (ξ, ζ) and Fig. 3 shows the contours of the displacement (equi-deformation curves) at some times. Figures 4 and 5 are for that of the step pulse load.

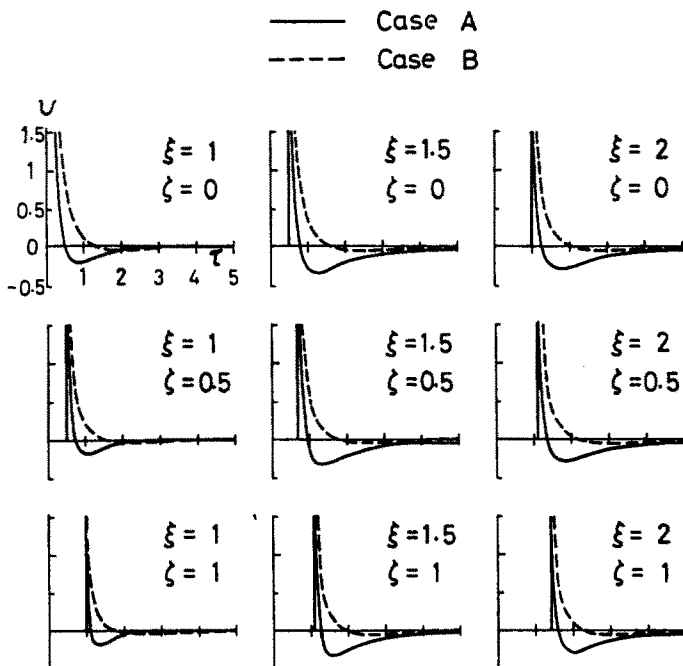


Fig. 2. Displacement response to an impulsive load.

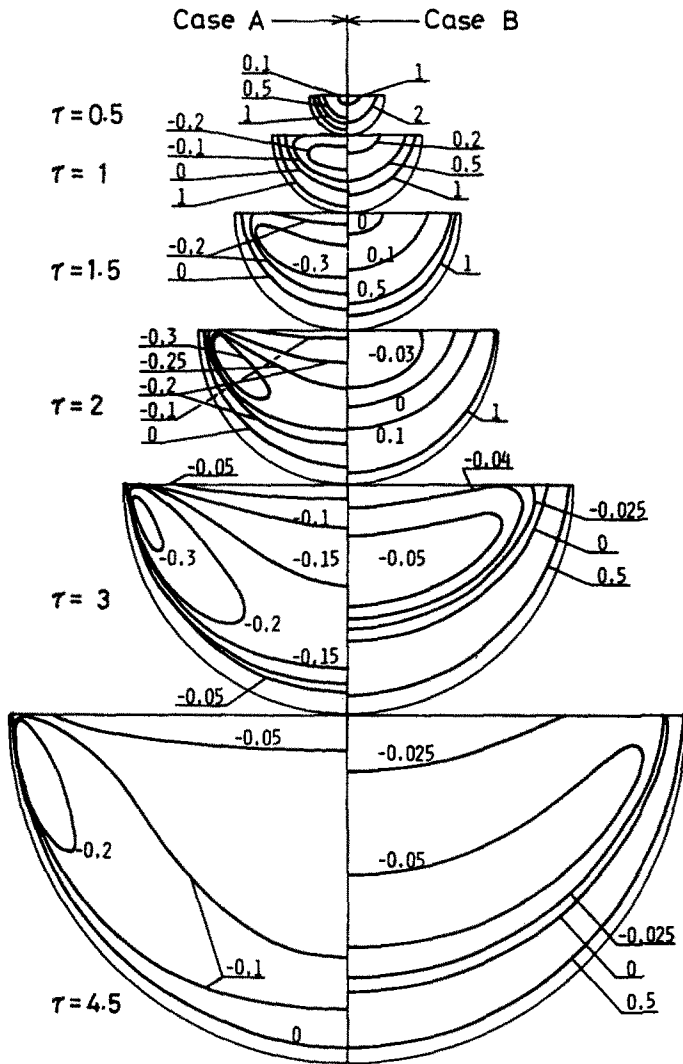


Fig. 3. Displacement contours for an impulsive load.

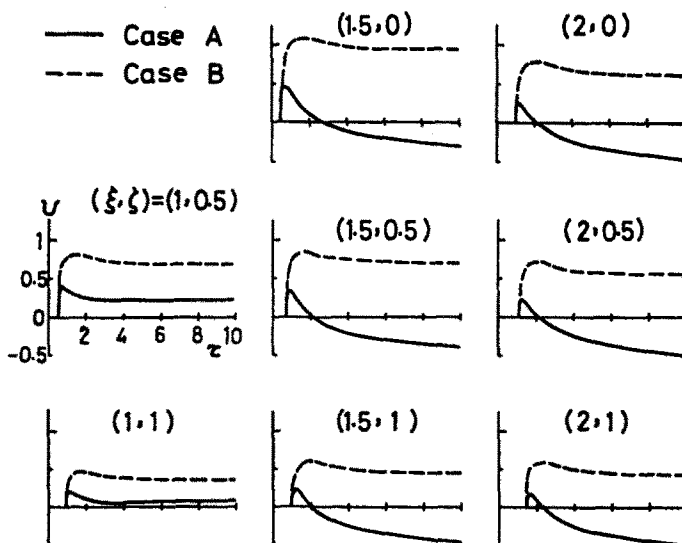


Fig. 4. Displacement response to a step pulse load.

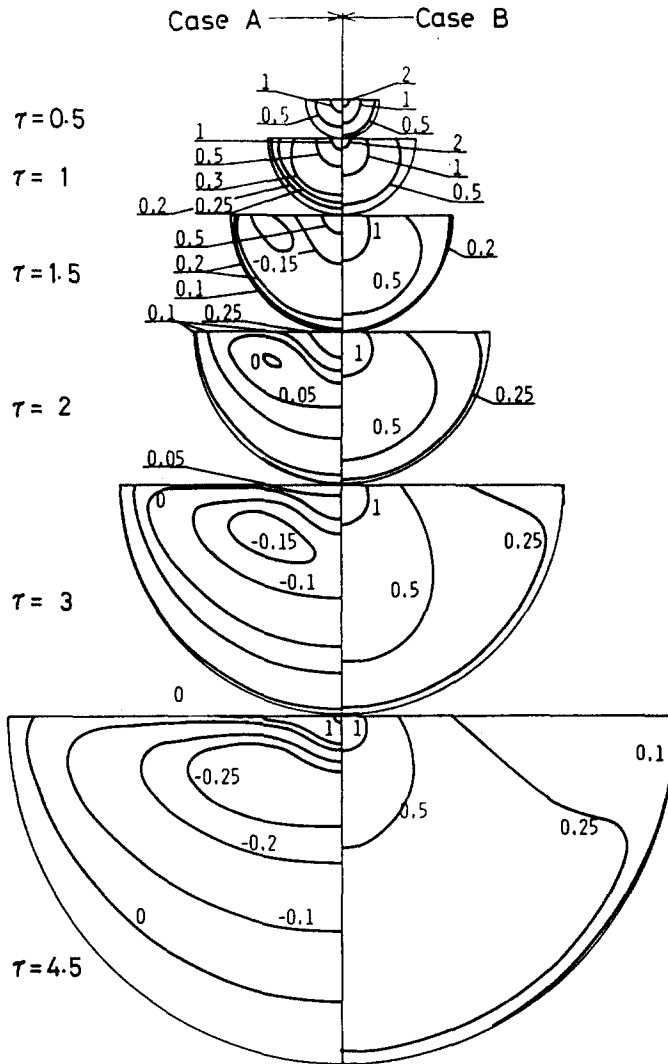


Fig. 5. Displacement contours for a step pulse load.

Because of the symmetry of the deformation, the contours in Figs. 3 and 5 are one-sided. Numerals in these figures are the values of the dimensionless displacement. From these figures we find that the response in Case A is more complex than that in Case B. It is interesting that a valley of the deformation is found only in Case A. The valley is formed near the shallow wave front in the case of the impulsive load. On the other hand, the valley in that of the step pulse load is far from the wave front.

The computations for the case of the moving load are carried out in three sub-cases according to the moving velocity;

- | | |
|--------------------------------|-----------|
| (c - 1) subseismic velocity: | $M = 0.5$ |
| (c - 2) seismic velocity: | $M = 1$ |
| (c - 3) superseismic velocity: | $M = 2.$ |

Results are shown in Figs. 6-11. From Figs. 6, 8 and 10, we can find that the difference in the displacement between Cases A and B becomes clearer as depth ξ increases, and that it fades out with increasing of Mach number M . Thus we can conclude that the inhomogeneity of the elastic solid has less effects on the response as the velocity of the moving load is greater. It should be pointed out that the deformation valley is also found

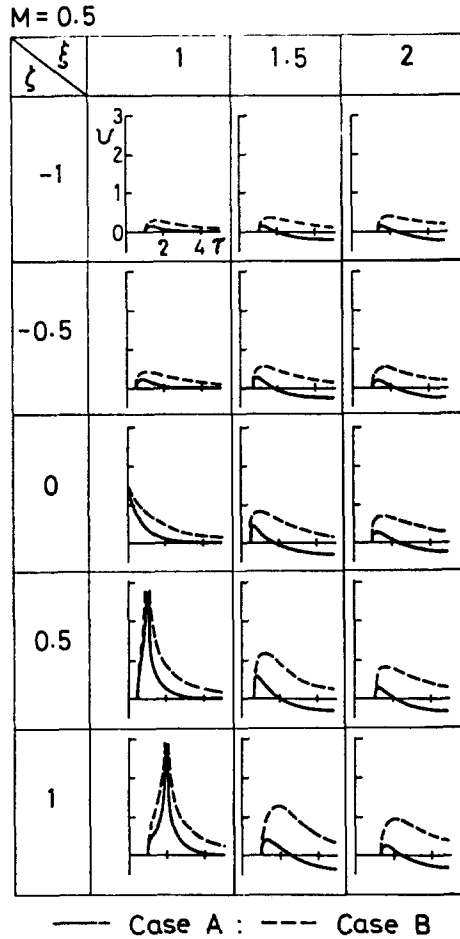


Fig. 6. Displacement response to a subseismically moving load.

only in Case A. But, the valley is not recognized before $\tau = 1$. After this time the valley appears and then transits toward the wave front of surface side. When the load moves superseismically, the valley does not appear in the leading wave region. In this region the contour in Case B is parallel to the leading wave front. As was in the case of the stationary load, the deformation in Case A is more complex than that in Case B.

WAVE FRONT SINGULARITY

It is preferable to discuss the wave front singularity for the transient problem of dynamic load.

A wave front, whose cross section is semi-circular, emanates from an initial point of the load and is defined by $\tau = R_0$. Extracting the singular term from each of eqns (48) to (50), we get

(a) *Impulsive load*

$$-\frac{\pi\mu_0}{F_0} U_{\theta j} \sim \frac{C_j}{\sqrt{2R_0}} \frac{1}{\sqrt{\Delta\tau}} \tag{62}$$

(b) *Step pulse load*

$$-\frac{\pi\mu_0}{F_0} U_{\theta j} \sim C_j \frac{2}{R_0} \sqrt{\Delta\tau} \tag{63}$$

(c) *Moving load*

$$-\frac{\pi\mu_0}{F_0}U_{\theta j} \sim \frac{\sqrt{2R_0}}{|\tau - M\zeta|} C_j \sqrt{\Delta\tau} \tag{64}$$

where

$$\Delta\tau = \tau - R_0. \tag{65}$$

When the load moves superseismically, the leading wave appears and its front is defined by $\tau = \tau^*$. Across this front a finite jump occurs.

$$-\frac{\pi\mu_0}{F_0}U_{\theta j} \sim C_j \frac{\pi}{\sqrt{M^2 - 1}}; \tau \rightarrow \tau^*. \tag{66}$$

Recalling eqn (36), we find that the jump in Case A decreases monotonically with increasing of the radial distance, but that the jump in Case B is constant.

Finally, the displacement singularity beneath the loaded point is derived for the case of the moving load. ($c - 1$) subseismic velocity;

$$-\frac{\pi\mu_0}{F_0}U_{\theta j} \sim -\frac{C_j}{\sqrt{1 - M^2}} \log |\Delta\zeta|. \tag{67}$$

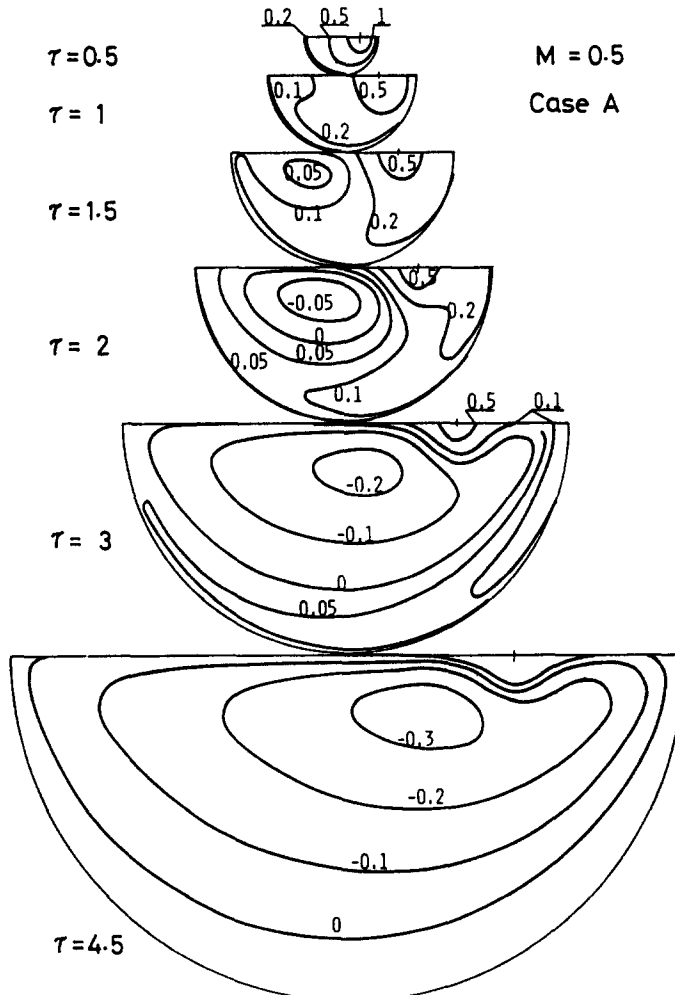


Fig. 7(a). Displacement contours for a subseismically moving load (Case A; $\lambda = 1$).

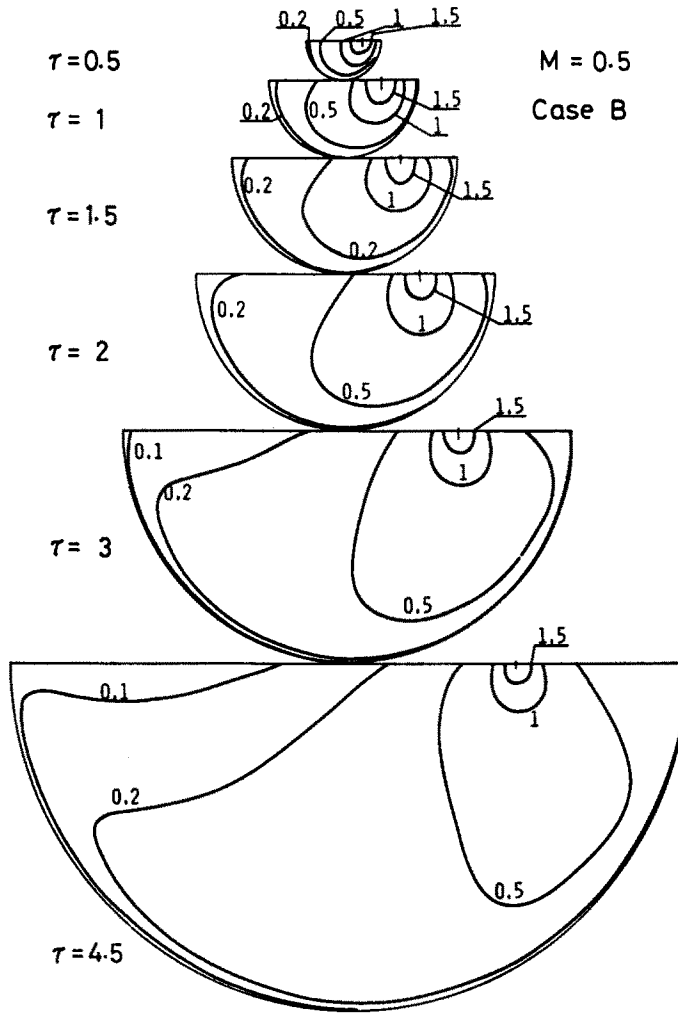


Fig. 7(b). Displacement contours for a subseismically moving load (Case B; $\lambda = -1$).

(c - 2) seismic velocity;

$$-\frac{\pi\mu_0}{F_0} U_{\theta j} \sim C_j \sqrt{\frac{2\zeta}{\Delta\zeta}}. \tag{68}$$

(c - 3) superseismic velocity;

$$-\frac{\pi\mu_0}{F_0} U_{\theta j} \sim C_j \frac{\pi}{\sqrt{M^2 - 1}} \tag{69}$$

where

$$\Delta\zeta = \tau - M\zeta. \tag{70}$$

CONCLUDING REMARKS

The transient response of an inhomogeneous elastic solid to a moving torsional ring load is discussed. Two cases of its inhomogeneity are considered.

A solution procedure is developed for a moving load of arbitrary motion and a general

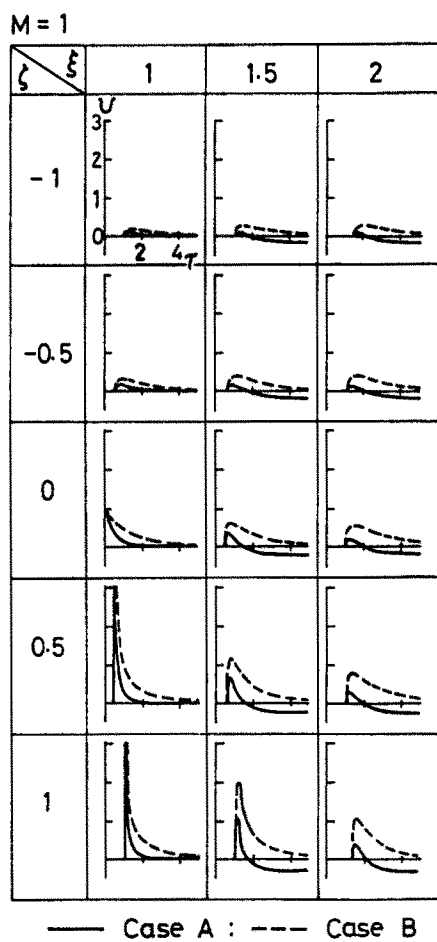


Fig. 8. Displacement response to a seismically moving load.

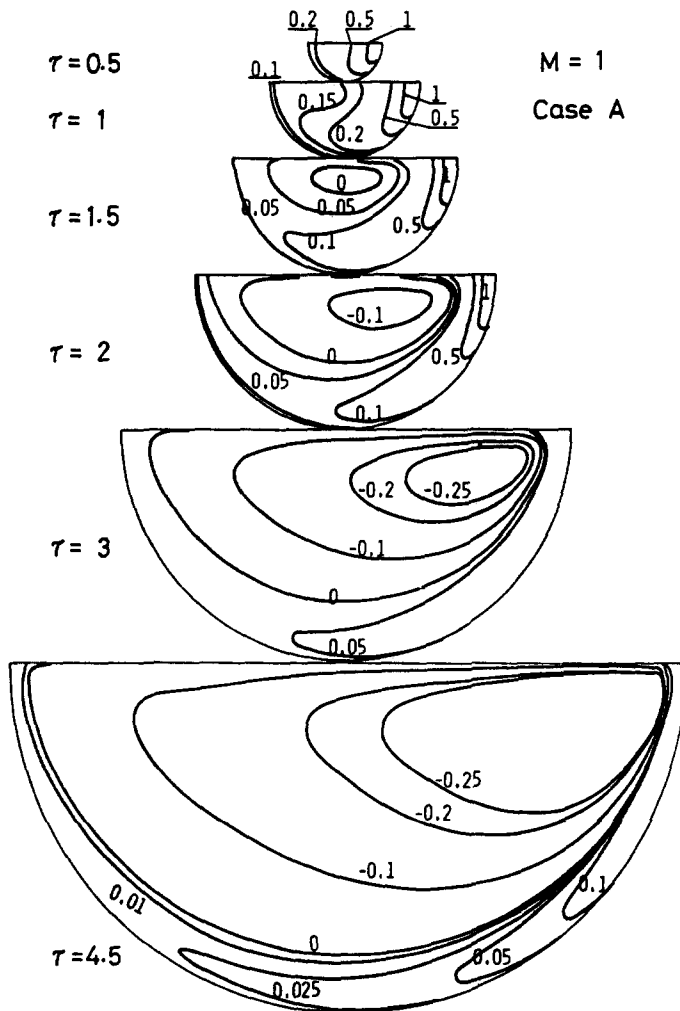


Fig. 9(a). Displacement contours for a seismically moving load (Case A; $\lambda = 1$).

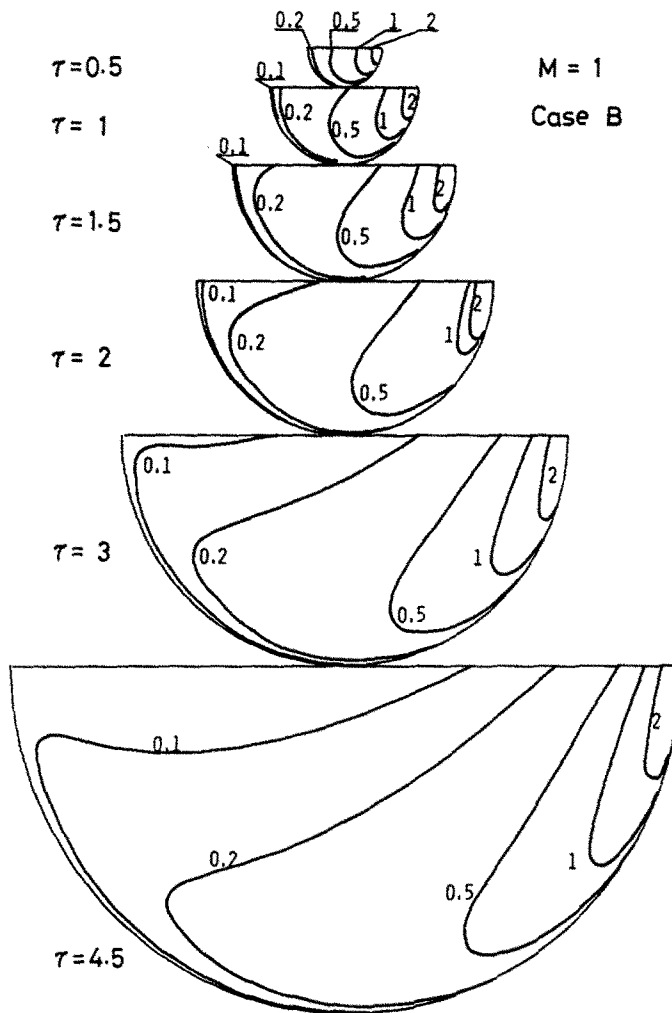


Fig. 9(b). Displacement contours for a seismically moving load (Case B; $\lambda = -1$).

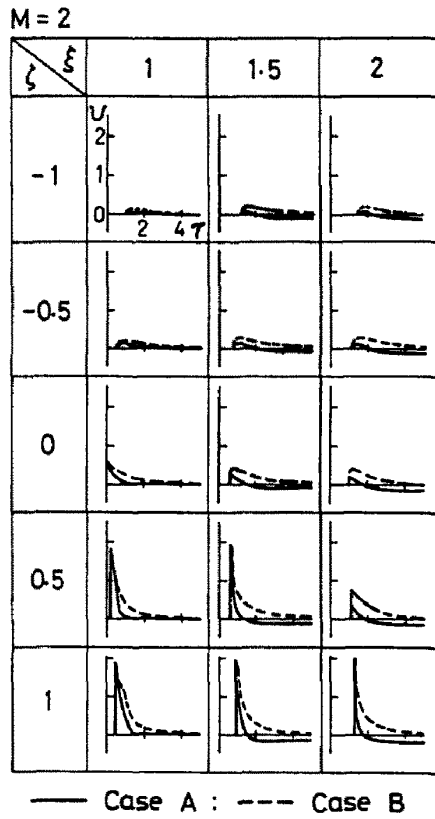


Fig. 10. Displacement response to a superseismically moving load.

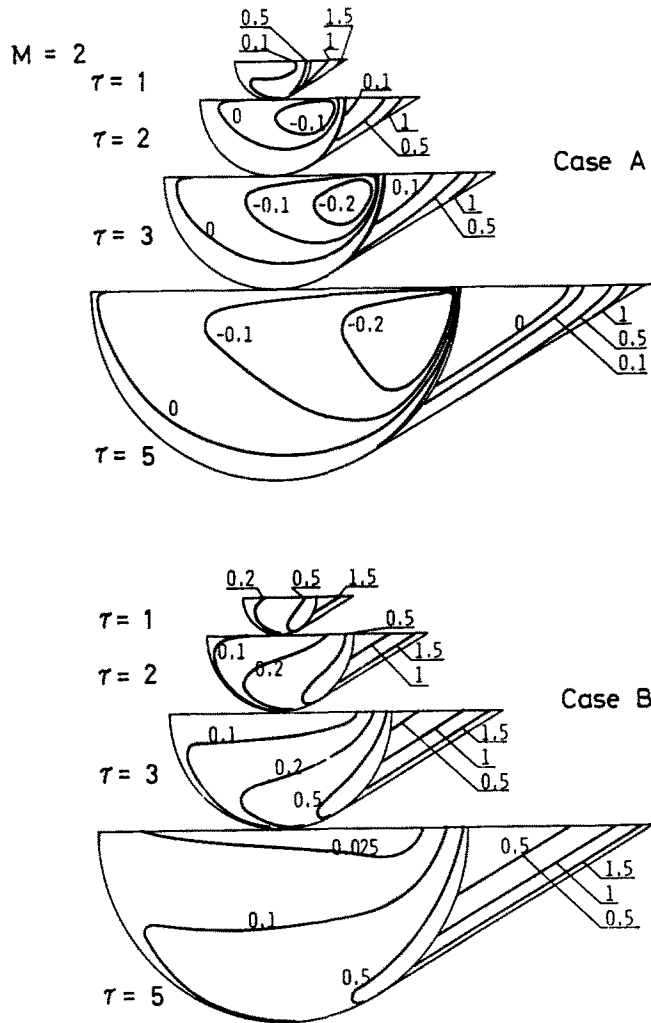


Fig. 11. Displacement contours for a superseismically moving load.

form of the solution is obtained. The solution is applicable to both transient and steady-state problems of the load. For the three cases of the loading the explicit expressions of the solution are derived. Numerical computations are carried out for the displacement in detail.

It is shown that the effect of the inhomogeneity is not so clear in the response as the load moves superseismically. When both the rigidity and the density increase with the radial distance (Case A), a valley of the deformation appears. The singularities at the wave fronts and beneath the loaded point are discussed. The jump across the leading wave front is constant in Case B, but it in Case A decreases with the radial distance as the load moves superseismically.

Acknowledgement—The author wishes to express his heartfelt thanks to Prof. A. Atsumi of Tohoku University for his guidances and encouragements throughout the work.

REFERENCES

1. R. Parnes, Response of an infinite elastic medium to traveling loads in a cylindrical bore. *Trans. ASME, Series. E, J. Appl. Mech.* **36**, 51–58 (1969).
2. R. Parnes, Progressing torsional loads along a bore in an elastic medium. *Int. J. Solids Structures* **16**, 653–670 (1980).
3. G. N. Watson, *Theory of Bessel Functions*, 2nd Edn. Cambridge (1966).
4. K. Watanabe, Transient response of an inhomogeneous elastic half-space to a torsional load. *Bull. JSME* **24**, 1537–1542 (1981).
5. K. Watanabe, Transient response of an infinite elastic solid to a moving point load. *Bull. JSME* **24**, 1115–1122 (1981).